Journal of Fluorescence, Vol. 8, No. 3, 1998

Influence of Torsional Vibrations on the Photoluminescence Characteristics of Dye Solutions

T. Marszałek[1]

Received January 23, 1998; Revised July 8, 1998; Accepted July 21, 1998

The influence of torsional vibrations of fluorophore molecule on polarization spectra and absorption/emission vibronic band profiles of isotropic dye solutions has been considered. Basing on the concept of luminescence center (LC) and assuming that (1) electronic transitions in the LC may be assisted by torsion-vibrational excitations, and (2) reorientations of the LC can be described in terms of Stokes–Einstein rotational diffusion, the formula for time-dependent emission anisotropy, $r(\tilde{\nu}_a, \tilde{\nu}_f, t)$ as a function of excitation, $\tilde{\nu}_a$, and observation, $\tilde{\nu}_f$, frequencies has been obtained. It comprises depolarization by combined reorientations of the fluorophore molecule, i.e., its torsional vibrations with respect to the LC, and rotational diffusion of the LC. This approach is a generalization of the appropriate results obtained earlier by Ehrenberg and Rigler and, independently, by Chuang and Isenthal. The considered model has specific property that the torsional vibrations appear both as depolarizing factor for $r(\tilde{\nu}_a, \tilde{\nu}_f, t)$ and as shaping factor for absorption/emission bands, resulting in the variation of the emission anisotropy across appropriate band profiles. This is demonstrated graphically using numerical results obtained for a simplified, one-dimensional torsional oscillator. It is also shown that observed absorption and emission spectra of coumarin solutions can be reproduced using this model with appropriate potentials for restoring forces.

KEY WORDS: Torsional vibrations; vibronic band profiles; emission anisotropy.

INTRODUCTION

It has long been recognized that the photoluminescence polarization technique is an important tool in the investigations of many physical and photochemical processes occurring in condensed molecular systems, such as isotropic (liquid and rigid) dye solutions, macroscopically ordered crystalline phases, phospholipid membranes, and others. The extensive review of problems and applied methods of photoluminescence polarization technique can be found in many review articles, books, treatises, and proceedings [1–14], to mention only a few, more recent. In particular, the polarization of the photoluminescence contains information on the reorientational dynamics of the dye molecules in solution. Convenient and commonly accepted quantitative measure of the polarization of photoluminescence of isotropic dye solutions is the emission anisotropy (EA),

$$r = \frac{I_\parallel - I_\perp}{I_\parallel + 2I_\perp} = \frac{3I_\parallel}{2I} - \frac{1}{2} \tag{1}$$

introduced by Jabłoński [15,16] in 1960. The $I_\parallel$ and $I_\perp$ are intensities of components of emission polarized in parallel and perpendicular directions respectively to the electric vector of linearly polarized exciting light beam, and $I = I_\parallel + 2I_\perp$ is the total intensity. In the case of transition between two nondegenerate electronic states, the value of the EA at time t after excitation by a very

[1] Institute of Physics, N. Copernicus University, ul. Grudziądzka 5, 87-100 Toruń, Poland.

1053-0509/98/0900-0229$15.00/0

short light pulse is given by

$$r(t) = \frac{3}{5}\langle\cos^2\beta(t)\rangle - \frac{1}{5} = \frac{2}{5}\langle D_{00}^{(2)}(0,\beta(t),0)\rangle \quad (2)$$

which is known as Perrin's formula [17]. $\beta(t)$ in Eq. (2) represents the angle between directions of the absorption dipole moment at time of excitation ($t = 0$) and the emission dipole moment at time t after excitation. $D_{mn}^{(L)}(\Omega)$ is the Wigner rotation matrix element—Rose's convention [18] is used throughout this work. The angular brackets denote ensemble averaging.

The time course of $r(t)$ is related to the processes randomizing the initially anisotropic (due to photoselection) orientation distribution of excited fluorophores. Examples of such processes are thermal reorientations (including restricted), excitation energy transfer, and others.

Theoretically allowed $r_0 = r(t = 0)$ values are confined, according to Eq. (2), to the interval 0.4 to -0.2, the upper limit corresponding to the colinear emission and absorption transition dipole moments and the lower limit to the mutually perpendicular orientations of these two vectors.

The aim of this paper is to investigate the effect of the torsional vibrations of dye molecules on the emission anisotropy characteristics (r_0 values, polarization spectra) and on the electronic absorption and emission band profiles.

The concept of the torsional vibrations was introduced first by Perrin [19] and then developed in the series of papers by Jabłoński [20–24] and others [25–29]. Jabłoński's interest in the torsional vibration initiated from the observation that the theoretically allowed limiting values of EA (0.4 and -0.2) were never obtained experimentally. This fact could be understood with the assumption that the emission and absorption transition moments of the dye molecule undergo limited fast (beyond experimental time resolution power) reorientations, leading to the apparent angular dispersion of these two vectors around their mean directions. Other possible explanations to these observations are discussed by Steinberg [30].

The impulse for considering anew the old problems relating the photoluminescence characteristics of dye solutions to torsional vibrations came from the series of recently published papers [31–34] concerning the shape of electronic absorption and emission spectra of dye solutions as interpreted by new concept of quasi-molecule. It follows from these publications that the oscillation modes of the dye molecule with respect to the surroundings is an important factor influencing the electronic absorption and emission band profiles. It is reasonable to assume that these oscillations (in general complicated) can be decomposed into two kinds of mutually independent simpler oscillations—translational (periodic center of mass movement without rotation) and rotational (periodic change of molecular orientations). This second kind of molecular motion (possibly highly irregular in solutions) will be called after Jabłoński [20,21], torsional vibrations. Note that under this kind of molecular oscillations, the absorption and emission transition dipole moments should also change their directions in time, following (more or less) the molecular movement. This is in contrast with internal molecular oscillations, which, due to the angular momentum conservation principle, do not change fluorophore orientations. Consequently this kind of oscillation does not influence directions of the appropriate transition moments, leading to the EA remaining independent of the absorption light frequency across the absorption band, and independent of the emission light frequency across the emission band, unless the Condon (crude Born–Oppenheimer adiabatic, according to the classification given in Table II of Ref. 35) approximation is inadequate, or some other frequency-dependent depolarizing mechanisms are involved.

We assume in this work that the electronic transitions can be assisted by the quanta of the torsional vibration excitations, contributing to the absorption, $\mathcal{A}(\tilde{\nu}_a)$, and emission, $\mathcal{F}(\tilde{\nu}_f)$ electronic band profiles, where $\tilde{\nu}_a$ and $\tilde{\nu}_f$ are absorption and emission (fluorescence) light frequencies. If that is the case, then the extent of depolarization by torsional vibrations should be dependent directly on $\tilde{\nu}_a$ and $\tilde{\nu}_f$. Selecting the value of $\tilde{\nu}_a$ is connected with the selection of appropriate vibrational energy levels, i.e., also the amplitude of the vibrations. The same applies to the $\tilde{\nu}_f$ values. In the result the angular dispersions of the absorption and emission transition moments should be dependent on $\tilde{\nu}_a$ and $\tilde{\nu}_f$ appropriately, making the EA also dependent on these frequencies, i.e., $r = r(\tilde{\nu}_a, \tilde{\nu}_f)$. This idea seems to a new contribution to the fluorescence depolarization problem, never analyzed (according to the author's knowledge) before.

Torsional vibrations, if they occur, are performed under the influence of some restoring forces acting between the dye molecule and its local surroundings. In these circumstances it is reasonable to assume that the polarization of photoluminescence of the dye solution is determined by the properties of objects composed of the fluorophore molecules and their nearest surroundings. We refer to such objects as luminescence centers (LC). A detailed description of the model of luminescence center considered in this work is given in Section 2.

When the LC as a whole can perform reorientations, for example, Brownian rotations occurring in liquid solution, then the total (i.e., with respect to the laboratory coordinate system) reorientation movement of the fluorophore is composed of two movements—the torsional vibration superimposed with the LC motion. The approach presented in this paper takes into account these two kinds of reorientations.

The structure of the paper is as follows. In the following section the model considered is described in some details. The subsequent section contains the mathematical formulation, and final equations obtained for the EA in time-resolved polarization experiments and experiments performed under stationary excitation. In the last section some numerical examples with relations to the absorption, $\mathcal{A}(\tilde{\nu}_a)$, and emission, $\mathcal{F}(\tilde{\nu}_f)$, band profiles are presented.

DESCRIPTION OF THE MODEL

The simplified model of the luminescence center used to describe the EA behavior of a fluorophore in dilute solution is given below. Its main features coincide with the quasi-molecular (or configuration coordinate) model [31–34,36–39] with emphasis on elucidation of the effects of torsional vibration movement. It is also close to the model considered by Moffit and Moscowitz [40] to describe the optical activity of absorbing media.

The absorption–emission cycle in general involves the following.

(1) Photon absorption–the process (with time duration of the order of 10^{-15} s) originating in the equilibrated ground electronic LC state and ending in the nonequilibrated exited electronic LC state (Franck–Condon state).

(2) After excitation of the LC three processes start to occur simultaneously.
- Population redistribution of the vibrational energy levels (in the excited LC), leading from an initially nonequilibrium to an equilibrium distribution (relaxation time, $\tau_v \approx 10^{-11}$–10^{-12} s).
- Adaptation of the excited LC to different (compared to the ground state) charge distributions in the fluorophore. This process involves solvation shell rearrangement (the appropriate relaxation time is viscosity dependent and takes values from $\tau_r = \infty$ for rigid solutions to $\tau_r \ll \tau_f$ for low-viscous solutions). After completing these two processes the LC is left in the equilibrated electronic excited state. To avoid unnecessary complications with dynamic Stokes shift and related dependence of the EA on observation light frequency, the considerations of this work are limited to two extreme cases: $\tau_r \ll \tau_f$ (low-viscous solutions) and $\tau_r \gg \tau_f$ (rigid solutions), with $\tau_v \ll \tau_f$ in each case.
- Radiative and nonradiative transitions to the ground Franck–Condon LC state (characteristic time duration of these processes, $\tau_f \approx 5$ ns—fluorescence decay time).

The equilibrated LC states are supposed to have the following properties.

a. Each LC consists of the fluorophore molecule inside a solvation shell composed of an (almost) rigid matrix of solvent molecules.

b. The luminescence centers are geometrically similar to one another, and their reorientations in liquid solution can be described in terms of Brownian rotations of an (in general) asymmetric rigid body, represented by the appropriate diffusion tensor in the Strokes–Einstein model.

c. The reorientational degrees of freedom for the fluorophore inside the LC appear as torsional modes of low fundamental frequencies, whose restoring forces can be described in terms of the interaction potential between the fluorophore and its surroundings. The torsion vibrational movement of the fluorophore is supposed to be much faster then the Brownian reorientations of the LC.

d. The vibronic wave functions of the LC, $\Psi_{giv}(x, q, Q)$ and $\Psi_{ei'v'}(x, q, Q)$, in the ground and excited electronic states of the fluorophore are sufficiently well approximated by a two-step Born–Oppenheimer adiabatic approximation [41,42], developed to describe the influence of the solvent on the vibronic spectra of dye molecules. Applying the procedure given in Ref. 42 to the system characterized by points a and c, one gets

$$\Psi_{giv}(x,q,Q) = \psi_{gi}(x,q,\underline{Q})\,\chi_{giv}(Q) \tag{3}$$

$$\Psi_{ei'v'}(x,q,Q) = \psi_{ei'}(x,q,\underline{Q})\,\chi_{ei'v'}(Q) \tag{4}$$

where x and q represent electron and nuclear coordinates (of the fluorophore). Q is, in general, a set of coordinates determining the localization and orientation of the fluorophore (as a whole) with respect to fixed in the LC coordinate system. Translational degrees of freedom do not, however, influence the emission anisotropy, so below we neglect translations, and Q is understood as orientational coordinates of M with respect to the LC.

$\psi_{gi}(x, q, Q)$ and $\psi_{ei'}(x, q, Q)$ are molecular Born–Oppenheimer (BO) adiabatic wave functions of the fluorophore molecule, obtained by taking into account its interaction with surroundings at fixed Q coordinates (coordinates appearing as slow-varying parameters are indicated by underlining). The appropriate vibronic fluorophore energy levels,

$$E_{gi} = E_{gi}(Q) \quad \text{and} \quad E_{ei'} = E_{ei'}(Q) \tag{5}$$

(i and i' labeling internal oscillation energy levels in the ground, g, and the excited, e, electronic states of the fluorophore) are dependent on the Q coordinates that are supposed to be slow-varying in time as compared to the x and q coordinates. Functions (5) appear as an (effective) interaction potential in the next step of the BO approximation leading to the equation for $\chi_{giv}(Q)$,

$$[\hat{T}(Q) + E_{gi}(Q)]\,\chi_{giv}(Q) = E_{giv}\,\chi_{giv}(Q) \tag{6}$$

and similarly for $\chi_{ei'v'}$. $\hat{T}(Q)$ in Eq. (6) is the kinetic energy operator of the fluorophore molecule approximated as a rigid body. The $\chi_{giv}(Q)$ and $\chi_{ei'v'}(Q)$ are wave functions describing the torsional vibration modes of the fluorophore inside the LC. They are labeled by υ and υ' to distinguish them from the internal modes of fluorophore oscillations (labeled by i and i'), which are supposed to have much higher fundamental frequencies. Using Eqs. (3) and (4) the vibronic transition (electric) dipole moment may be represented as

$$\vec{m}_{gi,ei'}(\underline{Q}) = \langle \psi_{gi}(x,q,\underline{Q}) \mid \vec{m}(x,q,\underline{Q}) \mid \psi_{ei'}(x,q,\underline{Q}) \rangle_{x,q} \tag{7}$$

For the absorption/emission spectral intensity distributions we adopt the formulae given by Lax [38]. In the case of unpolarized light we have [compare Eqs. (2.1), (2.2),(3.4), and (3.6) in Ref 38]:

$$I_{ei'gi}(\tilde{\nu}_a) = K_a \tilde{\nu}_a \int |\vec{m}_{ei',gi}(Q)|^2 P_{gi}(Q)\, \delta(\Delta E_{ei',gi}(Q) - \tilde{\nu}_a)\, dQ \tag{8}$$

for absorption and

$$I_{gj,ej'}(\tilde{\nu}_f) = K_e \tilde{\nu}_f^3 \int |\vec{m}_{gj,ej'}(Q)|^2 P_{ej'}(Q)\, \delta(\Delta E_{ej',gj}(Q) - \tilde{\nu}_f)\, dQ \tag{9}$$

for emission. $P(Q)$ in (8) and (9) are the quantum-statistical mechanical probability distributions for the orientation Q of the fluorophore with respect to the LC frame. For the considered model they are given by

$$P_{gi}(Q) = AV_\upsilon |\chi_{giv}(Q)|^2, \qquad P_{ej'}(Q) = AV_{\upsilon'} |\chi_{ej'\upsilon'}(Q)|^2 \tag{10}$$

where AV represents averaging over initial, v (or v') states weighted with the appropriate Boltzmann factors. $\Delta E(Q)$ is equal to

$$\Delta E_{ei',gi}(Q) = E_{ei'}(Q) - E_{gi}(Q) \tag{11}$$

for absorption, and similarly for emission, where $E(Q)$ are the effective Born–Oppenheimer potentials in the appropriate ground and excited states [compare Eqs. (5) and (6)]. Equations (8) and (9) represent a good approximation when many initial states, v in the case of absorption and v' in the case of emission, are involved in transition (with given $\tilde{\nu}_a$), and the final states for transitions have large quantum numbers υ' and υ appropriately.

The main purpose of this work is to elucidate the effects of torsional vibrations on polarization and other spectral properties of dye solutions. Having this in mind, we concentrate our attention on transitions with arbitrary but fixed internal vibration quantum numbers, i, i', j, j', and only υ and υ' allowed to vary. To simplify assignments, all the indices i, i', j, j', will be further postponed. In addition, we adopt the following assignments for transition moments:

$$\vec{a}(Q) \quad \left[\text{instead of } \vec{m}_{ei',gi}(Q)\right] \quad \text{for absorption} \tag{12}$$

and

$$\vec{f}(Q) \quad \left[\text{instead of } \vec{m}_{gj,ej'}(Q)\right] \quad \text{for emission} \tag{13}$$

Both i, i' in (12) and j', j in (13) are understood as arbitrary but fixed quantum numbers. Their values refer in general to different parts of spectra and can be adjusted, for example, to the vicinity of maxima of the absorption and emission bands.

EMISSION ANISOTROPY. MATHEMATICAL FORMULATION

We consider the time-resolved polarization experiment in the typical (usually rectangular) experimental configuration, with a resolution time of the order of 10^{-10}–10^{-11}. The sample is excited at $t = 0$ by a very short pulse of light polarized with an electric vector along the $z^{(L)}$ axis (L, laboratory Cartesian axes system) and having $\tilde{\nu}_a$ frequency. The fluorescence intensity at $\tilde{\nu}_f$ frequency and polarization along, ($I_\parallel$), or perpendicular to ($I_\perp$), the $z^{(L)}$ axis is probed at time t after excitation.

We start our considerations by evaluating I and $I_{\parallel}$ in Eq. (1). In the frame of the semiclassical approach, the probability of photon absorption [with $\tilde{\nu}_a$ frequency and along the $z_{(L)}$ axis polarization] by a particular (single) LC is proportional to [compare Eq. (8)]

$$\tilde{\nu}_a \int |\vec{a}(Q)|^2 \cos^2 (z^L, a(Q)) P_g (Q) \delta (\Delta E_{e,g}(Q) - \tilde{\nu}_a) dQ$$

the emission probability per unit time [with $\tilde{\nu}_f$ frequency and polarization along the $z^{(L)}$ axis] is proportional to

$$\tilde{\nu}_f^3 \int |\vec{f}(Q)|^2 \cos^2 (z^L, f(Q)) P_e (Q) \delta (\Delta E_{e,g} (Q) - \tilde{\nu}_f) dQ$$

and the total (i.e., without selection of polarization) emission probability is proportional to

$$\tilde{\nu}_f^3 \int |\vec{f}(Q)|^2 P_e (Q) \delta (\Delta E_{e,g} (Q) - \tilde{\nu}_f) dQ$$

The appropriate intensities of the emission in Eq. (1) refer to the whole ensemble of the LCs in the sample and are then given by

$$I(\tilde{\nu}_a, \tilde{\nu}_f, t) = \tilde{\nu}_a \tilde{\nu}_f^3 CK (t) \left\langle \left[\int |\vec{a} (Q)|^2 \cos^2 (z^L, a(Q))_{t=0} P_g (Q) \delta (\Delta E_{e,g} (Q) - \tilde{\nu}_a) dQ \right] \times \left[\int |\vec{f} (Q')|^2 P_e (Q') \delta (\Delta E_{e,g} (Q') - \tilde{\nu}_f) dQ' \right] \right\rangle \quad (14)$$

$$I_{\parallel}(\tilde{\nu}_a, \tilde{\nu}_f, t) = \tilde{\nu}_a \tilde{\nu}_f^3 CK (t) \left\langle \left[\int |\vec{a} (Q)|^2 \cos^2 (z^L, a(Q))_{t=0} P_g (Q) \delta (\Delta E_{e,g} (Q) - \tilde{\nu}_a) dQ \right] \times \left[\int |\vec{f} (Q')|^2 \cos^2 (z^L, f(Q'))_t P_e (Q') \delta (\Delta E_{e,g} (Q') - \tilde{\nu}_f) dQ' \right] \right\rangle \quad (15)$$

where C is a constant, $K(t)$ is the decay function of excited LCs, $\Delta E_{eg}(Q) = E_e(Q) - E_g(Q)$ and similarly for $\Delta E_{eg}(Q')$, $\delta(\Delta E_{eg}(Q) - \tilde{\nu}_a)$ and $\delta(\Delta E_{eg}(Q') - \tilde{\nu}_f)$ ensure that only transitions with appropriate energy separations contribute to the selected frequencies $\tilde{\nu}_a$, $\tilde{\nu}_f$, and the angular brackets denote ensemble averaging over all orientations of the LCs in two indicated time moments.

The ensemble averaging is conveniently performed using the Wigner rotation matrix formalism. In particular, first replacing the cosine square in Eq. (14) by $^1/_3$ (1 + $2D_{00}^{(2)}$ ($\Omega_{L\to a}$)) and then expanding the term $D_{00}^{(2)}$ ($\Omega_{L\to a}$) according to the closure theorem, we get

$$\cos^2 (z^{(L)}, a) = \frac{1}{3} (1 + 2 \sum_{i=-2}^{2} D_{0i}^{(2)*} (\Omega_{L\to LC}) D_{i0}^{(2)*} (\Omega_{LC\to a})) \quad (16)$$

Similarly, for $\cos^2(z^{(L)}, f)$, in Eq. (15), i.e.,

$$\cos^2 (z^{(L)}, f) = \frac{1}{3} (1 + 2 \sum_{j=-2}^{2} D_{0j}^{(2)} (\Omega'_{L\to LC}) D_j^{(2)} (\Omega'_{LC\to f})) \quad (17)$$

The following assignments have been introduced. $D_{mn}^{(2)}$ ($\Omega_{I\to J}$) are second-rank Wigner rotation matrix elements; $\Omega_{I\to J} = (\alpha_{I\to J}, \beta_{I\to J}, \gamma_{I\to J})$ are Euler angles that determine the orientation of the J Cartesian axis system with respect to the I Cartesian axis system, where I, J are laboratory (L), luminescence center (LC), molecular (M), and transition moment $\vec{a}$, $\vec{f}$ subunits. By Ω' the appropriate orientation at observation time, t, is understood, while Ω refers to the orientation at $t = 0$, i.e., at the time of excitation. The z axes of the coordinate systems attached to the individual $\vec{a}$, $\vec{f}$ vectors are oriented along the vector directions. The LC axes are oriented along principal axes, D_1, D_2, D_3, of the LC diffusion tensor, and the M axes are oriented along the principal axes of the molecular moment of inertia tensor.

After inserting Eq. (16) into Eq. (14), and Eqs. (16) and (17) into Eq. (15), we can see that the following ensemble averages have to be evaluated:

(a) $\langle D_{0i}^{(2)*} (\Omega_{L\to LC}) \rangle$, (b) $\langle D_{0j}^{(2)} (\Omega'_{L\to LC}) \rangle$,

(c) $\langle D_{0i}^{(2)*} (\Omega_{L\to LC}) D_{0j}^{(2)} (\Omega'_{L\to LC}) \rangle$

The ensemble averages a–c are readily obtained using Green's function, $G(\Omega, 0|\Omega', t)$, representing the conditional probability that the object of interest has, at time t, orientation Ω', if at $t = 0$ its orientation was Ω. Green's function for rotational diffusion in an isotropic solution can be represented by (see, for example, Refs. 43 and 44)

$$G(\Omega, 0|\Omega', t) = \sum_{p=0}^{\infty} \frac{2p + 1}{8\pi^2} \sum_{k,m,s,r=-p}^{p} \exp (-\varepsilon_k^{(p)} t) a_{ks}^{(p)*} D_{ms}^{p} (\Omega) a_{kr}^{(p)} D_{mr}^{(p)*} (\Omega') \quad (18)$$

where $a_{ki}^{(p)}$ and $\varepsilon_k^{(p)}$ are constant coefficients, first given by Favro [45] and later used in Refs. 43, 44, 46, and 47. It turns out that only coefficients with the $p = 2$ superscript come into the final equations. For quick reference they are tabulated in Appendix A, based on the Huntress paper [43]. Note that all $a_{ki}^{(2)}$ and $\varepsilon_k^{(2)}$ are real variables.

The ensemble average is given by

$$\langle X(\Omega,\Omega',t)\rangle = \frac{1}{8\pi^2}\int\int X(\Omega,\Omega',t)\, G(\Omega, 0|\Omega',t)\, d\Omega\, d\Omega' \tag{19}$$

Based on Eqs. (18) and (19) and taking into account orthogonality of the Wigner matrix elements,

$$\int D^{(p)}_{mn}(\Omega)\, D^{(p')}_{m',n'}{}^{*}(\Omega)\, d\Omega = \frac{8\pi^2}{2p+1}\,\delta_{p,p'}\,\delta_{m,m'}\,\delta_{n,n'} \tag{20}$$

one obtains

$$\langle D^{(2)}_{0i}{}^{*}(\Omega_{L\to LC})\rangle = \langle D^{(2)}_{0j}(\Omega'_{L\to LC})\rangle = 0 \tag{21}$$

for all i and j, and

$$\langle D^{(2)}_{0i}{}^{*}(\Omega_{L\to LC})\, D^{(2)}_{0j}{}^{*}(\Omega'_{L\to LC})\rangle = \frac{1}{5}\sum_{k=-2}^{2}\exp(-\varepsilon^{(2)}_k t)\, a^{(2)}_{ki}{}^{*}\, a^{(2)}_{kj} \tag{22}$$

Inserting now Eqs. (14) and (15) into Eq. (1), one can derive, after some rearrangements taking into account results (16), (17), (21) and (22),

$$r(\tilde{\nu}_a, \tilde{\nu}_f, t) = \sum_{k=-2}^{2} C_k(\tilde{\nu}_a, \tilde{\nu}_f)\exp(-\varepsilon^{(2)}_k t) \tag{23}$$

where

$$C_k(\tilde{\nu}_a, \tilde{\nu}_f) = \frac{2}{5}\sum_{i,j=-2}^{2} a^{(2)}_{ki}{}^{*}\, B^{*}_i(\tilde{\nu}_a)\, a^{(2)}_{kj}\, B_j(\tilde{\nu}_f); \quad k = 0, \pm 1, \pm 2 \tag{24}$$

with

$$B^{*}_i(\tilde{\nu}_a) = \frac{\int |\vec{a}(Q)|^2\, D^{(2)}_{j0}{}^{*}(\Omega_{LC\to a(Q)})\, P_g(Q)\,\delta(\Delta E_{e,g}(Q) - \tilde{\nu}_a)\, dQ}{\int |\vec{a}(Q)|^2\, P_g(Q)\,\delta(\Delta E_{e,g}(Q) - \tilde{\nu}_a)\, dQ} \tag{25}$$

$$B_j(\tilde{\nu}_f) = \frac{\int |\vec{f}(Q')|^2\, D^{(2)}_{j0}(\Omega'_{LC\to f(Q')})\, P_e(Q')\,\delta(\Delta E_{e,g}(Q') - \tilde{\nu}_f)\, dQ'}{\int |\vec{f}(Q')|^2\, P_e(Q')\,\delta(\Delta E_{e,g}(Q') - \tilde{\nu}_f)\, dQ'} \tag{26}$$

The Wigner matrix elements $D^{(2)*}_{i0}$ and $D^{(2)}_{j0}$ appearing in Eqs. (25) and (26) can be expanded, using closure theorem, into

$$D^{(2)}_{i0}{}^{*}(\Omega_{LC\to a(Q)}) = \sum_{m=-2}^{2} D^{(2)}_{im}{}^{*}(\Omega_{LC\to M})\, D^{(2)}_{m0}{}^{*}(\Omega_{M\to a(Q)}) \tag{27}$$

$$D^{(2)}_{j0}(\Omega'_{LC\to f(Q')}) = \sum_{n=-2}^{2} D^{(2)}_{jn}(\Omega'_{LC\to M})\, D^{(2)}_{n0}(\Omega'_{M\to f(Q')}); \; i,j = 0, \pm 1, \pm 2 \tag{28}$$

where $\Omega_{LC\to M}$ and $\Omega'_{LC\to M}$ have the same meaning as Q and Q' appropriately, i.e., $\Omega_{LC\to M} \equiv Q$, $\Omega'_{LC\to M} \equiv Q'$ (compare section under Description of the Model). Note that the orientations $\Omega_{M\to a(Q)}$ and $\Omega'_{M\to f(Q')}$ appearing in $D^{(2)*}_{m0}$ and $D^{(2)}_{n0}$ are given in a form indicating explicitly that the vectors $\vec{a}$ and $\vec{f}$ may not be, in general, rigidly fixed in the M frame. This is consistent with the quantum mechanical approach and is related to the variation of interaction strength between the fluorophore molecule and its surroundings when the orientation Q varies.

Equation (23) is a generalization of the result given by Ehrenberg and Rigler [see Eq. (3.23) in Ref. 46] and the equivalent result obtained by Chuang and Isenthal [47], both relating to single absorption and emission transition dipole moments, rigidly attached to the fluorophore molecule undergoing reorientations due to rotational diffusion only. In such a case Eq. (23) reduces to the appropriate results of the Refs. 46 and 47. This is readily seen after identifying the LC with M by setting $\Omega_{LC\to M} = \Omega'_{LC\to M} = 0$, and assuming that vectors $\vec{a}$, $\vec{f}$ are Q-independent. Under these conditions [and remembering that $D^{(2)}_{pq}(\Omega = 0) = \delta_{pq}$)], the Eqs, (25) and (26) reduce appropriately to

$$B^{*}_i = D^{(2)}_{i0}{}^{*}(\Omega_{LC\to a}), \qquad B_j = D^{(2)}_{j0}(\Omega_{LC\to f})$$

which, after insertion into Eq. (24), leads to C_k becoming identical to C^2_{k0} given by Eqs. (3.24) in Ref. 46. In terms of C^2_{k0} the EA becomes, at $t = 0$,

$$r_0 = \sum_{k=-2}^{2} C^2_{k0} = \frac{2}{5}\sum_{i,j=-2}^{2}\sum_{k=-2}^{2} a^{(2)}_{ki}\, D^{(2)}_{i0}{}^{*}\, a^{(2)}_{kj}\, D^{(2)}_{j0}$$

and since (compare Appendix A)

$$\sum_{k=-2}^{2} a^{(2)}_{ki}\, a^{(2)}_{kj} = \delta_{ij} \tag{29}$$

can be reduced to [compare Eq. (2)]

$$r_0 = \frac{2}{5}\sum_{i=-2}^{2} D^{(2)}_{i0}{}^{*}(\Omega_{LC\to a})\, D^{(2)}_{i0}(\Omega_{LC\to f}) = \frac{2}{5} D^{(2)}_{00}(\Omega_{a\to f}) \tag{30}$$

If the directions of the two vectors $\vec{a}$ and $\vec{f}$ with respect to the molecular frame are independent of the internal oscillation modes of the fluorophore molecule (as in the case of the Condon approximation), then r_0 given by Eq. (30) is independent of the frequency $\tilde{\nu}_f$ across the emission band, and also independent of the excitation frequency, $\tilde{\nu}_a$, across the absorption band.

The generalized (to include effects of torsional vibrations) Eq. (23) leads to a somewhat different behavior of r_0. From Eqs. (23), (24), and (29) we get

$$r_0 = \sum_{k=-2}^{2} C_k(\tilde{\nu}_a, \tilde{\nu}_f) = \frac{2}{5} \sum_{i=-2}^{2} B_i^*(\tilde{\nu}_a) B_i(\tilde{\nu}_f) \quad (31)$$

with B_i^* and B_i being frequency-dependent weighted averages (25) and (26) of the Wigner matrix elements $C_{i0}^{(2)*}(\Omega_{LC\to a})$ and $D_{i0}^{(2)}(\Omega_{LC\to f})$ overall accessible due to torsional vibration orientations of $\vec{a}$ and $\vec{f}$ with respect to the LC. The angular spreading of the transition moments, over some solid angles in the LC, makes the r_0 values given by Eq. (31) different from—in most cases lower (in absolute values) than—those given by Eq. (30). This explains, in accordance with the suggestion expressed long ago by Jabloński [21], the rarity of the experimental appearance of the values $r_0 = 0.4$ and $r_0 = -0.2$. Moreover, according to Eq. (31) r_0 is dependent on the frequencies $\tilde{\nu}_a$ and $\tilde{\nu}_f$.

At the end of this section let us complete the general Eq. (23) by two special cases corresponding to axially symmetric and spherical rotors. For axially symmetric rotors, $D_x = D_y = D_\perp$, $D_z = D_\parallel$, and (see Appendix A) $\varepsilon_0^{(2)} = 6D_\perp$, $\varepsilon_1^{(2)} = \varepsilon_{-1}^{(2)} = 5D_\perp + D_\parallel$, $\varepsilon_2^{(2)} = \varepsilon_{-2}^{(2)} = 2D_\perp + 4D_\parallel$, leading to

$$r(\tilde{\nu}_a, \tilde{\nu}_f, t) = C_0 e^{-6D_\perp t} + (C_1 + C_{-1}) e^{-(5D_\perp + D_\parallel)t} + (C_2 + C_{-2}) e^{-(2D_\perp + 4D_\parallel)t} \quad (32)$$

with

$$C_0 = \frac{2}{5} B_0^*(\tilde{\nu}_a) B_0(\tilde{\nu}_f)$$

$$C_1 + C_{-1} = \frac{2}{5}(B_1^*(\tilde{\nu}_a) B_1(\tilde{\nu}_f) + B_{-1}^*(\tilde{\nu}_a) B_{-1}(\tilde{\nu}_f)) \quad (33)$$

$$C_2 + C_{-2} = \frac{2}{5}(B_2^*(\tilde{\nu}_a) B_2(\tilde{\nu}_f) + B_{-2}^*(\tilde{\nu}_a) B_{-2}(\tilde{\nu}_f))$$

For spherical rotors, $D_x = D_y = D_z = D$, and $\varepsilon_k^{(2)} = 6D$ for $k = 0, \pm 1, \pm 2$, leading to

$$r(\tilde{\nu}_a, \tilde{\nu}_f, t) = r_0(\tilde{\nu}_a, \tilde{\nu}_f) \exp(-6Dt) \quad (34)$$

with r_0 given by Eq. (31). The value of the EA under stationary excitation is

$$\overline{r(\tilde{\nu}_a, \tilde{\nu}_f, t)} = \frac{\int_0^\infty r(t) K(t)\, dt}{\int_0^\infty K(t)\, dt} \quad (35)$$

where $K(t)$ is the excited-state decay function.

SIMPLIFICATIONS. NUMERICAL EXAMPLE

Equation (23)–(28) and (31) for the EA are accurate in the framework of the considered simplified model of the LC, but functions appearing there are rather complicated, making it difficult to get quick insight into the form of the $r_0(\tilde{\nu}_a, \tilde{\nu}_f)$ dependence. For this purpose further simplifications can be helpful.

One such difficulty arises from the possibility (mentioned in the previous section) that the directions of the transition moments, $\vec{a}$ and $\vec{f}$, may not be, in general, fixed in the fluorophore frame M, i.e., their rotations may not follow exactly the fluorophore torsional motion in the LC. To take this phenomenon into consideration, the solution of a complicated quantum-mechanical problem is required. It is not undertaken in this work. Instead we apply in this section the commonly used approximation that the disturbances imposed on $\vec{a}$ and $\vec{f}$ from the external environment are negligible, and the values and directions of these two vectors can be regarded as being rigidly fixed in the fluorophore frame (i.e., Q-independent with respect to the M frame).

Under this approximation we obtain, after inserting Eq. (27) into (25) and Eq. (28) into (26),

$$B_i^*(\tilde{\nu}_a) = \frac{\sum_{m=-2}^{2} D_{m0}^{(2)*}(\Omega_{M\to a}) \int D_{im}^{(2)*}(Q) P_g(Q) \delta(\Delta E_{e,g}(Q) - \tilde{\nu}_a)\, dQ}{\int P_g(Q) \delta(\Delta E_{e,g}(Q) - \tilde{\nu}_a)\, dQ} \quad (36)$$

$$B_j(\tilde{\nu}_f) = \frac{\sum_{n=-2}^{2} D_{n0}^{(2)}(\Omega_{M\to f}) \int D_{jn}^{(2)}(Q) P_e(Q) \delta(\Delta E_{e,g}(Q) - \tilde{\nu}_f)\, dQ}{\int P_e(Q) \delta(\Delta E_{e,g}(Q) - \tilde{\nu}_f)\, dQ} \quad (37)$$

For $P(Q)$ the Boltzmann population distribution functions

$$P_g(Q) = \exp\left(-\frac{E_g(Q)}{kT}\right),$$

$$P_e(Q) = \exp\left(-\frac{E_e(Q) - E_e(Q^{(0)})}{kT}\right) \quad (38)$$

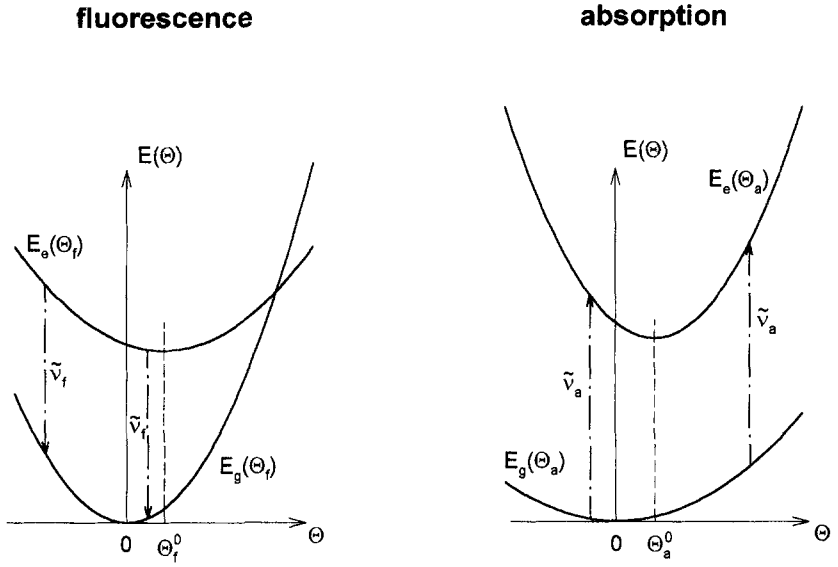

Fig. 1. Configurations of the restoring potentials [Eqs. (42), (43)] for torsional vibrations of the fluorophore molecule in the ground, $E_g(\Theta)$, and excited, $E_e(\Theta)$, electronic states. The vertical arrows represent two vibronic transitions with the same frequency, $\tilde{\nu}_f$, in the fluorescence band (left) and two vibronic transitions with the same frequency, $\tilde{\nu}_a$, in the absorption band (right).

in the appropriate states can be used (compare Refs. 31–34), representing an approximation applicable when absorption (emission) transitions start from sufficiently high vibrational energy levels υ, (υ'), as occurs in the case of oscillations with low fundamental frequencies, $\hbar\omega \ll kT$. Note that the denominators in Eqs. (36) and (37) with $P(Q)$ given by Eqs. (38) coincide (formally) with the equations used in Refs. 31–34 to describe absorption, $\mathcal{A}(\tilde{\nu}_a)$, and emission, $\mathcal{F}(\tilde{\nu}_f)$, band profiles, i.e.,

$$\frac{\mathcal{A}(\tilde{\nu}_a)}{\tilde{\nu}_a} = \mathcal{A}_0 \int P_g(Q)\, \delta(\Delta E_{e,g}(Q) - \tilde{\nu}_a)\, dQ \quad (39)$$

$$\frac{\mathcal{F}(\tilde{\nu}_f)}{\tilde{\nu}_f^3} = \mathcal{F}_0 \int P_e(Q)\, \delta(\Delta E_{e,g}(Q) - \tilde{\nu}_f)\, dQ \quad (40)$$

[compare, for example, Eqs. (8)–(11) in Ref. 34].

Based on Eqs. (36)–(38) we consider in some detail the simple case of one-dimensional torsional vibrations, and estimate numerical values of r_0 for different values of frequencies $\tilde{\nu}_a$ and $\tilde{\nu}_f$.

Suppose that the fluorophore molecule performs one-dimensional torsional oscillation around its $y^{(M)}$ axis, being the principal axis of the inertial tensor. Let $y^{(M)}$ coincide (for simplicity) with the $y^{(LC)}$ axis of the luminescence center. In terms of the Eulerian angles, the orientation of the M system with respect to the LC system is then given as

$$Q \equiv \Omega_{LC\to M} = (0, \Theta, 0) \quad (41)$$

Assume now that the oscillations are harmonic, i.e., restoring forces are given by the potential

$$E_g(\Theta) = k_\alpha \Theta^2 \quad (42)$$

in the electronic ground state and

$$E_e(\Theta) = k'_\alpha (\Theta - \Theta_\alpha^{(0)})^2 + b_\alpha \quad (43)$$

in the excited state, with α = a for absorption, and α = f for emission (fluorescence) process (see Fig. 1). The difference between the sets of parameters for these two processes is related to the fact that each of them involves different pairs of quantum states, as mentioned in the preceding section. The parameters appearing in Eqs. (42) and (43) have the following meanings.

- k_α, k'_α Parameters determining the restoring forces responsible for the torsional vibrations of the fluorophore in the electronic ground and excited state, respectively,
- b_α Energy difference between the minima of the potential energies $E_e(\Theta_\alpha^{(0)})$ and $E_g(0)$ (b_α = energy of 0–0 transition).

$\Theta_\alpha^{(0)}$ The coordinate localizing the minimum potential energy in the excited state, ($\Theta = \Theta_\alpha^{(0)}$), with respect to the appropriate minimum in the ground state ($\Theta = 0$); the minima of the two potentials are allowed to be localized at different coordinates, due, for example, to different, in general, values and directions of the permanent dipole moments in the ground and excited states.

The introduced simplifications are probably far from reality (particularly the limitation to one-dimensional torsional oscillations), nevertheless, they are helpful in estimating numerical values of the considered effects of torsional vibrations on polarization spectra and to reveal tendencies of their behavior. Under these simplifications all integrals appearing in Eqs. (36)–(40) can be solved analytically. The details of calculations and form of the resulting functions $B_i^*(\tilde{\nu}_a)$, $B_j(\tilde{\nu}_f)$, $\mathcal{A}(\tilde{\nu}_a)$, and $\mathcal{F}(\tilde{\nu}_f)$ are given in Appendix B.

The dependence of r_0 on $\tilde{\nu}_a$, $\tilde{\nu}_f$ frequencies, as obtained based on these B functions, is illustrated in Figs. 2a and b (solid-line curves). Calculations have been performed for $\vec{a} \| \vec{f}$, both vectors lying in the plane perpendicular to the rotation axis, $y^{(M)}$, i.e., with $\Omega_{M \to a/f} = (0, \vartheta, 0)$. The resulting absorption, $\mathcal{A}(\tilde{\nu}_a)$, and emission, $\mathcal{F}(\tilde{\nu}_f)$, band profiles (i.e., obtained under the assumption that solely one-dimensional torsional vibration is a profile-making factor) are also indicated in Figs. 2a and b, after normalization to 1 at maximum. Calculations of $\mathcal{A}(\tilde{\nu}_a)$ and $\mathcal{F}(\tilde{\nu}_f)$ have been performed with

$$\begin{aligned} c_a &= 640\ \text{cm}^{-1}, & d_a &= 2000\ \text{cm}^{-1}, \\ b_a &= 25{,}714\ \text{cm}^{-1} & c_f &= 1750\ \text{cm}^{-1}, \\ c_f' &= 670\ \text{cm}^{-1}, & b_f &= 24{,}000\ \text{cm}^{-1}, \\ T &= 293\ \text{K} \end{aligned} \tag{44}$$

i.e., values that are close to those determined experimentally in Refs. 31 and 33 for ethanolic solutions of coumarin 2 at $T = 293$ K. Two additional parameters, $\Theta_a^{(0)}$ and $\Theta_f^{(0)}$, that are required for $r_0(\tilde{\nu}_a, \tilde{\nu}_f)$ calculations have been assumed to be

$$\Theta_a^{(0)} = 0.2\text{rad}, \qquad \Theta_f^{(0)} = 0.23\text{rad}, \tag{45}$$

for results presented in Fig. 2a

$$\Theta_a^{(0)} = \Theta_f^{(0)} = 0.3\text{rad} \tag{46}$$

for results presented in Fig. 2b

Values (45) for $\Theta_\alpha^{(0)}$ together with values (44) for c_α, c'_α correspond to the following values of k_α, k'_α and energy $\varepsilon^{tors} = h\nu^{tors}$ of fundamental torsional frequencies (ν^{tors}) [see Eqs. (B6) and (B7) in Appendix B]:

$$\begin{aligned} k_a &= 16{,}000\ \text{cm}^{-1}, & \varepsilon_a^{tors} &= 24.4\ \text{cm}^{-1}, \\ &\text{in the equilibrated ground state} \\ k_a' &= 50{,}000\ \text{cm}^{-1}, & \varepsilon_\alpha^{'tors} &= 43.2\ \text{cm}^{-1}, \\ &\text{in the excited Franck–Condon state} \\ k_f &= 33{,}080\ \text{cm}^{-1}, & \varepsilon_f^{tors} &= 35.2\ \text{cm}^{-1}, \\ &\text{in the Franck–Condon ground state} \\ k_f' &= 12{,}665\ \text{cm}^{-1}, & \varepsilon_f^{'tors} &= 21.7\ \text{cm}^{-1}, \\ &\text{in the equilibrated excited state} \end{aligned} \tag{47}$$

It can be seen the values of ε^{tors} are rather reasonable from the point of view of dynamical and spectroscopic properties of the considered model system.

Note that absorption and emission band profiles are represented by smooth continuous curves. This is a consequence of approximations lying under Eqs. (8) and (9) and their further simplifications made by replacing quantum-mechanical distribution [10] by classical functions [38]. The resulting final equations relate, in fact, to the classical Franck–Condon approximation, stating that electronic absorption/emission bands arise from vertical transitions between turning points on initial and final potential curves responsible for heavy particle movements. The $\Theta_\alpha^{\pm}(\tilde{\nu}_\alpha)$ [see Eq. (B5) in Appendix B] represent the positions of such turning points in torsional vibration motion of the fluorophore molecule.

Analyzing the results illustrated in Figs. 2a and b, first note that the normalized absorption and emission band profiles (dashed lines) are insensitive to the $\Theta_a^{(0)}$ and $\Theta_f^{(0)}$ values. This observation has been made earlier and it turned out to be very helpful in interpretation of the vibronic band profiles of some classes of dye solutions in condensed media [31–34]. Interpretation is based on the equations identical (in form) to (B8) and (B9) of this work, except that the Θ variable is understood as a coordinate representing all oscillation modes that contribute actively to band profiles.

Another two effects demonstrated by Fig. 2 are that (i) the limiting value of the emission anisotropy (r_0) clearly depends on the excitation ($\tilde{\nu}_a$) and fluorescence ($\tilde{\nu}_f$) frequencies, and (ii) the form of this dependence is influenced by the values of $\Theta_a^{(0)}$ and $\Theta_f^{(0)}$, in contrast with band profiles (which are not influenced by these parameters).

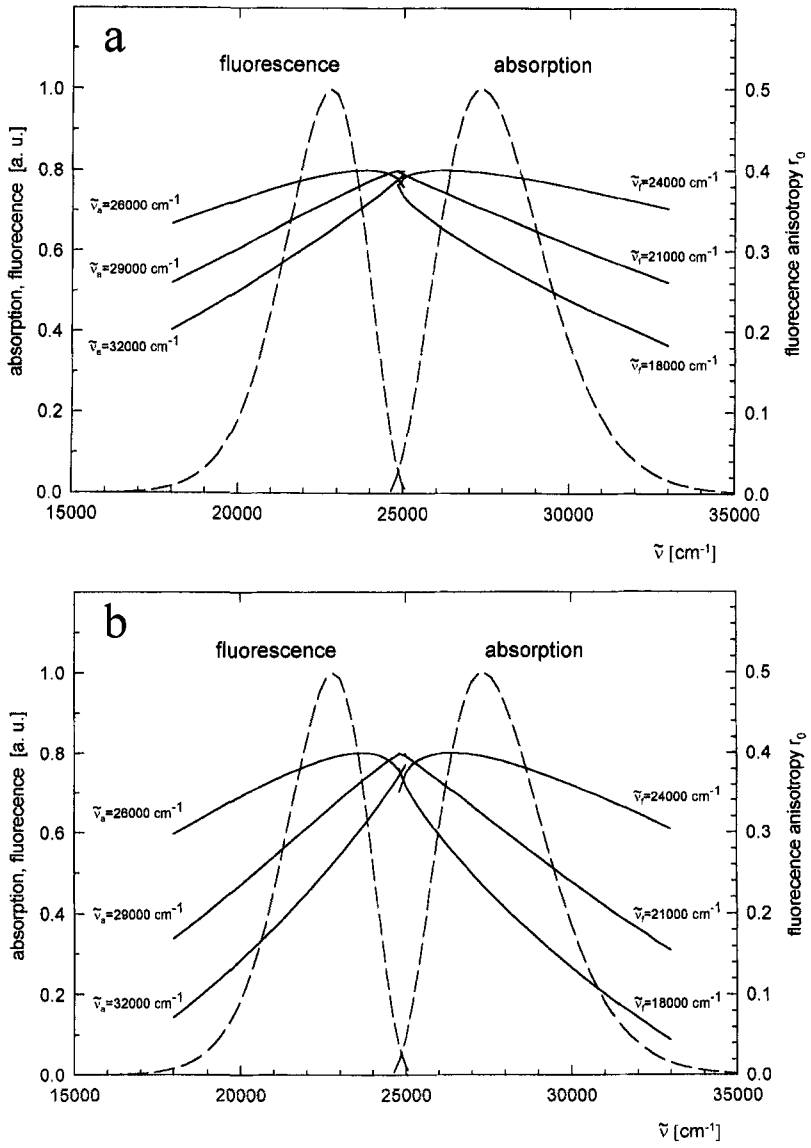

Fig. 2. Dependence of r_o on $\tilde{\nu}_f$ and $\tilde{\nu}_a$ frequencies (solid lines) across fluorescence and absorption band profiles (dashed lines). (a) $\Theta_a^{(0)} = 0.2$rad, $\Theta_f^{(0)} = 0.23$rad; (b) $\Theta_a^{(0)} = \Theta_f^{(0)} = 0.3$rad. The absorption and emission band profiles are obtained based on Eqs. (B8) and (B9). $r_o(\tilde{\nu}_a, \tilde{\nu}_f)$ is obtained based on Eq. (31) with Eqs. (B1) and (B2). Values of the b, c, c', and T parameters are taken from (44).

In the considered case of $\vec{a} \| \vec{f}$ (in the M frame) r_o comes close to 0.4 only when some specific relation between the two frequencies, $\tilde{\nu}_a$ and $\tilde{\nu}_f$, is fulfilled. This happens to take place when the absorption or emission (or both) frequency lies inside or is close to the absorption–fluorescence interception region. Beyond this region, r_o decreases with increasing $\tilde{\nu}_a$ and decreasing $\tilde{\nu}_f$ frequency. The steepness of the r_o decreases becomes greater with increasing (in reasonable limits) values of $\Theta_a^{(0)}$ and $\Theta_f^{(0)}$ (compare Figs. 2a and b). Intuitively such behavior is consistent with the "diffused" (due to torsional vibrations) oscillator model considered by Jabłoński. This time, however, the amplitude (i.e., also the energy) of torsions influences not only the values of angular spreading of vectors $\vec{a}$ and $\vec{f}$ but also becomes the shaping factor for vibronic, emission and absorption,

bands. It follows that the band profiles and polarization spectra contain overlapping (partially) information about the properties of the molecular system, suggesting that global analysis, comprising both kinds of (experimental) data, may be more successful than the analysis of each set of data separately. Limitations as to the applicability of appropriate equations in such an analysis should, however, be taken into account.

SUMMARY

The influence of torsional vibrations on polarization spectra of dye solutions has been analyzed based on the assumption that the torsional oscillations can assist in electronic transitions, contributing both to the absorption/emission vibronic band shapes and to the fluorescence depolarization. As a result, the emission anisotropy becomes dependent (directly) on the $\tilde{\nu}_a$ and $\tilde{\nu}_f$ frequencies across these bands.

The proposed mechanism seems to be a new contribution to the problem of EA behavior, leading to the $r(\tilde{\nu}_a, \tilde{\nu}_f)$ variation across the (single) bands. It differs from other, earlier recognized mechanisms, causing similar effects. Putting aside the trivial ones, we review below only the most fundamental mechanisms: (a) inadequacy of the Condon approximation [30,49,50]; (b) dynamic Stokes shift effect (see, for examples, Refs. 10, 14, and 48); and (c) shock effect [22] (see also Refs. 7, 14, and 48 and, for experimental verification, Refs. 25 and 26). Among these three, the shock effect contains some elements that are also present in the model discussed in this paper. In particular, in the shock effect approach, the decrease in the EA with increasing excitation frequency $\tilde{\nu}_a$ is accounted for by a sudden (jump -like) increase in the local temperature of the luminescence center, when the energy of the absorbed photon exceeds the 0–0 energy gap. Increases in the temperature intensify depolarizing, temperature-dependent effects, such as Brownian rotations and torsional vibrations. As a result, the torsional vibrations contribute to the $\tilde{\nu}_a$-dependent depolarization, but indirectly, in contrast to the suggestion discussed in this paper. In fact, all the frequency-dependent mechanisms mentioned above may appear simultaneously.

If torsional vibrations can assist in vibronic transitions, then selecting the frequencies $\tilde{\nu}_a$ and/or $\tilde{\nu}_f$) within appropriate bands is connected with the selection of the energy of torsional excitations, i.e., also their amplitudes, influencing the EA value. The role of the selecting machine is played by the Franck–Condon principle. To estimate the magnitude of such effects and to determine how they depend on the frequencies, the simple model of the LC (for details see Description of the Model) has been considered. The following properties of the LC are most important: (a) the LC creates appropriate conditions for torsional oscillations of the fluorophore molecule to occur (restoring potential can be introduced); (b) the torsional vibrations are rapid with respect to time resolution of the experiment and are also fast with respect to the characteristic reorientation time of the LC (the Brownian reorientations of the LC are allowed to account for depolarization by rotational diffusion in liquids); and (c) to elucidate effects of torsional vibrations the considerations are limited to the model case where solely torsional vibrations are the profile-making factor contributing to the absorption (emission) bands.

The results of calculations for the EA are summarized by Eq. (23) together with Eqs. (25)–(28) and approximated Eqs. (36), (37), and (38). The vibronic band profiles are given by the approximate Eqs. (39) and (40). It becomes clear from inspection of these equations [particularly Eqs. (25)–(28)] that there are mutual dependences between the $r(\tilde{\nu}_a, \tilde{\nu}_f)$ and the emission (absorption) band profiles. Graphical illustration of such interdependence is given in Fig. 2, presenting numerically obtained results for one-dimensional harmonic torsional oscillations. In spite of the simplifications introduced, the theoretical absorption and emission band profiles are able to reproduce experimental results for coumarin liquid solutions.

The physicochemical conditions in the real solutions may be very different from those assumed in calculations. Applicability of the obtained results is then dependent on the properties of a system under investigation. One can expect that the conditions of the fluorophore chemically attached to a large molecule (like a protein) may mimic quite closely the requirements of the LC model. The equations obtained could then be helpful in removing the effects of rapid (torsional) oscillations from polarization data, in structural and dynamical investigations of biological or phospholipid membrane structures. Adaptation of the model to such structures seems to be possible.

Finally, let us note that the absorption/emission bands of organic dye solutions, liquid and solid, are usually composed of many subbands, mutually overlapping in general. If each of these subbands is describable in terms of equations like [39], [40], i.e, arise from (nondepolarizing) vibronic transition broadened due to torsional vibrations, then determination of the r_o $(\tilde{\nu}_a, \tilde{\nu}_f)$ across the bands should be possible using appropriate combinations. It is clear that de-

polarization produced by torsional vibrations should be lower (then that demonstrated in Fig. 2) when many non-depolarizing transitions contribute to the emission anisotropy at given frequencies $\tilde{\nu}_a$, $\tilde{\nu}_f$. The dependence of r_o ($\tilde{\nu}_a$, $\tilde{\nu}_f$) across the complex bands may not follow the dependencies presented in Fig. 2.

APPENDIX A

Assignments in Table I are as follows.

$$\begin{aligned} a &= \sqrt{3}(D_x - D_y), \\ b &= 2D_z - D_x - D_y + 2\Delta, \\ D &= \frac{1}{3}(D_x + D_y + D_z) \\ \Delta &= (D_x^2 + D_y^2 + D_z^2 \\ &\quad - D_xD_y - D_xD_z - D_yD_z)^{\frac{1}{2}}, \\ N &= 2(b\Delta)^{\frac{1}{2}} \end{aligned} \tag{A1}$$

D_x, D_y, and D_z are the principal values of the diffusion tensor.

In the case of symmetric rotors, $D_x = D_y = D_\perp$, $D_z = D_\parallel$, one gets $a = 0$, $b = N = 4(D_\parallel - D_\perp)$, leading to $a_{ki}^{(2)}$ and $\varepsilon_k^{(2)}$ given in Table II.

Table I. Values of the Coefficients $a_{ki}^{(2)}$ and $\varepsilon_k^{(2)}$ for Asymmetric Rotors (After Ref. 49)[a]

k	$a_{k2}^{(2)}$	$a_{k1}^{(2)}$	$a_{k0}^{(2)}$	$a_{k,-1}^{(2)}$	$a_{k,-2}^{(2)}$	$\varepsilon_k^{(2)}$
2	$\frac{b}{\sqrt{2N}}$	0	$\frac{a}{N}$	0	$\frac{b}{\sqrt{2N}}$	$6D + 2\Delta$
1	0	$\frac{1}{\sqrt{2}}$	0	$\frac{1}{\sqrt{2}}$	0	$3(D + D_x)$
0	$-\frac{a}{\sqrt{2N}}$	0	$\frac{b}{N}$	0	$-\frac{a}{\sqrt{2N}}$	$6D - 2\Delta$
−1	0	$\frac{1}{\sqrt{2}}$	0	$-\frac{1}{\sqrt{2}}$	0	$3(D + D_y)$
−2	$\frac{1}{\sqrt{2}}$	0	0	0	$-\frac{1}{\sqrt{2}}$	$3(D + D_z)$

Table II. Values of the Coefficients $a_{ki}^{(2)}$ and $\varepsilon_k^{(2)}$ for Symmetric Rotors

k	$a_{k2}^{(2)}$	$a_{k1}^{(2)}$	$a_{k0}^{(2)}$	$a_{k,-1}^{(2)}$	$a_{k,-2}^{(2)}$	$\varepsilon_k^{(2)}$
2	$\frac{1}{\sqrt{2}}$	0	0	0	$\frac{1}{\sqrt{2}}$	$2D_\perp + 4D_\parallel$
1	0	$\frac{1}{\sqrt{2}}$	0	$\frac{1}{\sqrt{2}}$	0	$5D_\perp + D_\parallel$
0	0	0	1	0	0	$6D_\perp$
−1	0	$\frac{1}{\sqrt{2}}$	0	$-\frac{1}{\sqrt{2}}$	0	$5D_\perp + D_\parallel$
−2	$\frac{1}{\sqrt{2}}$	0	0	0	$-\frac{1}{\sqrt{2}}$	$2D_\perp + 4D_\parallel$

In both cases the $a_{ki}^{(2)}$ coefficients fulfill the relation

$$\sum_{k=-2}^{2} a_{ki}^{(2)} a_{kj}^{(2)} = \delta_{ij} \tag{A2}$$

which can be verified directly using Table I or Table II.

APPENDIX B

The integrals appearing in Eqs. (37), (38), (40), and (41) are evaluated using the formula $\int f(x)\delta(g(x))dx = \sum_i f(x_i)/|\frac{dg}{dx}|_i$, where x_i are roots of the equation $g(x) = 0$. On restoring potentials (43) and (44) and Θ_a^0, $\Theta_f^0 \neq 0$, one obtains

$$B_i^*(\tilde{\nu}_a) = \sum_{m=-2}^{2} D_{m0}^{(2)*}(\Omega_{M\to a}) \tag{B1}$$
$$\times \frac{D_{im}^{(2)*}(\Theta_a^{(+)}) \exp\left[-\frac{c_a}{kT}\left(\frac{\Theta_a^{(+)}}{\Theta_a^{(0)}}\right)^2\right] + D_{im}^{(2)*}(\Theta_a^{(-)}) \exp\left[-\frac{c_a}{kT}\left(\frac{\Theta_a^{(-)}}{\Theta_a^{(0)}}\right)^2\right]}{\exp\left[-\frac{c_a}{kT}\left(\frac{\Theta_a^{(+)}}{\Theta_a^{(0)}}\right)^2\right] + \exp\left[-\frac{c_a}{kT}\left(\frac{\Theta_a^{(-)}}{\Theta_a^{(0)}}\right)^2\right]}$$

$$B_j(\tilde{\nu}_f) = \sum_{n=2}^{2} D_{n0}^{(2)}(\Omega_{M\to f}) \tag{B2}$$
$$\times \frac{D_{jn}^{(2)}(\Theta_f^{(+)}) \exp\left[-\frac{c'_f}{kT}\left(\frac{\Theta_f^{(+)}}{\Theta_f^{(0)}} - 1\right)^2\right] + D_{jn}^{(2)}(\Theta_f^{(-)}) \exp\left[-\frac{c'_f}{kT}\left(\frac{\Theta_f^{(-)}}{\Theta_f^{(0)}} - 1\right)^2\right]}{\exp\left[-\frac{c'_f}{kT}\left(\frac{\Theta_f^{(+)}}{\Theta_f^{(0)}} - 1\right)^2\right] + \exp\left[-\frac{c'_f}{kT}\left(\frac{\Theta_f^{(-)}}{\Theta_f^{(0)}} - 1\right)^2\right]}$$

where the following assignments have been used:

$$c_\alpha = k_\alpha \Theta_\alpha^{(0)2}, \qquad c'_\alpha = k'_\alpha \Theta_\alpha^{(0)2} \tag{B3}$$

$$R_\alpha(\tilde{\nu}_\alpha) = \sqrt{c_\alpha c'_\alpha - (c'_\alpha - c_\alpha)(b_\alpha - \tilde{\nu}_\alpha)} \tag{B4}$$

$$\Theta_\alpha^{\pm}(\tilde{\nu}_\alpha) = \Theta_\alpha^{(0)} \frac{c'_\alpha \pm R_\alpha(\tilde{\nu}_\alpha)}{c'_\alpha - c_\alpha}, \qquad \alpha = a, f \tag{B5}$$

The $\Theta_\alpha^{\pm}(\tilde{\nu}_\alpha)$ represent turning points in the torsional motion of the fluorophore with respect to the LC frame.

The fundamental frequency ν^{tors} of this motion (rotational oscillations around fixed axis) is dependent on the constant k of the restorig potential and on the fluorophore moment of inertia I with respect to the axis of rotational oscillations, by the formula

$$\nu_\alpha^{\text{tors}} = \frac{1}{2\pi}\sqrt{(2k_\alpha)/I} \tag{B6}$$

The energy of the fundamental oscillations is given by

$$\varepsilon = h\nu^{\text{tors}} \tag{B7}$$

The moment of inertia of the coumarin 2 molecule with

respect to its shorter axis lying in the molecular plane has been estimated as $I_y^{(M)} = 3 \times 10^{-44}$ J s^2 = 1.51×10^{-21} cm $^{-1}$ s^2. The ε values given in Eq. (55) are obtained based on this value and appropriate k values.

The absorption and emission band profiles [Eqs. (40) and (41)] transform appropriately to

$$\mathcal{A}(\tilde{\nu}_a) = \frac{\mathcal{A}_0 \tilde{\nu}_a \Theta_a^{(0)}}{2R_A(\tilde{\nu}_a)} \left[\exp\left[-\frac{c_a}{kT}\left(\frac{\Theta_a^{(+)}}{\Theta_a^{(0)}}\right)^2\right] + \exp\left[-\frac{c_a}{kT}\left(\frac{\Theta_a^{(-)}}{\Theta_a^{(0)}}\right)^2\right]\right] \tag{B8}$$

$$\mathcal{F}(\tilde{\nu}_f) = \frac{\mathcal{F}_0 \tilde{\nu}_f \Theta_f^{(0)}}{2R_F(\tilde{\nu}_f)} \left[\exp\left[-\frac{c'_f}{kT}\left(\frac{\Theta_f^{(+)}}{\Theta_f^{(0)}} - 1\right)^2\right] + \exp\left[-\frac{c'_f}{kT}\left(\frac{\Theta_f^{(-)}}{\Theta_f^{(0)}} - 1\right)^2\right]\right] \tag{B9}$$

Inspection of Eqs. (B8) and (B9) leads to the conclusion that the functions $\mathcal{A}(\tilde{\nu}_a)$ and $\mathcal{F}(\tilde{\nu}_f)$, after normalization in maximum to some value (for example, to 1), become independent of the k's and $Q^{(0)}$ separately but dependent on their products c_α, c'_α and, obviously, on the b_α and T parameters

$$\alpha = a, f \tag{B10}$$

ACKNOWLEDGMENTS

I would like to thank Professor A. Baczyński for helpful and encouraging discussions and Dr. P. Targowski for assistance with numerical analysis. This work was supported by the Polish Government through KBN Grant 2 PO3B 124 09.

REFERENCES

1. A. Kawski (1983) *Photochem. Photobiol.* **38**, 487.
2. C. Zannoni, A. Arcioni, and P. Cavatorta (1983) in *Chemistry and Physics of Lipids*, Elsevier Scientific, Vol. **32**, pp. 179–250.
3. A. Kawski (1987) in *Progress and Trends in Applied Optical Spectroscopy* SOS 86, Bd. 13, Teubner Texte zur Physik, Leipzig, pp. 6–34.
4. R. E. Dale (1988) in B. Samori and E. W. Thulstrup (Eds.), *Polarized Spectroscopy of Ordered Systems*, NATO ASI, Series C (Mathematical and Physical Sciences), Kluwer, Dordrecht, The Netherlands, pp. 491–567.
5. A. Kawski (1989) in D. Fassler. (Ed.), *Optical Spectroscopy in Chemistry and Biology—Progress and Trends*, Verlag, Berlin, p. 135.
6. R. F. Steiner (1991) in J. R. Lakowicz (Ed.), *Topics of Fluorescence Spectroscopy, Vol. 2. Principles*, Plenum Press, New York, London, Chap. 1.
7. A. Kawski (1993) in *Crit. Rev. Anal. Chem.* **23**, 459–529.
8. Y. K. Levine and G. van Ginkel (1994) in G. R. Luckhurst and C. A. Veracini (Eds.), *The Molecular Dynamics of Liquid Crystals*, NATO ASI Series C (Mathematical and Physical Sciences), Kluwer, Dordrecht, The Netherlands, pp. 537–571.
9. R. B. Cundall and R. E. Dale (Eds.) (1983) *Time-Resolved Fluorescence Spectroscopy in Biochemistry and Biology*, NATO ASI Series A (Life Sciences), Plenum Press, New York.
10. J. R. Lakowicz (1983) *Principles of Fluorescence Spectroscopy*, Plenum Press, New York, Chaps. 5–6.
11. L. Brand, J. R. Knutson, L. Davenport, J. M. Beechem, R. E. Dale, D. G. Walbridge, and A. Kowalczyk (1985) in P. M. Bayley and R. E. Dale (Eds.), *Spectroscopy and the Dynamics of Molecular Biological Systems*, Academic Press, London, p. 259.
12. J. Michl and E. W. Thulstrup (1986) *Spectroscopy with Polarized Light. Solute Alignment by Photoselection, in Liquid Crystals, Polymers, and Membranes*, VCH, New York.
13. J. R. Lakowicz (Ed.) (1991) *Topics in Fluorescence Spectroscopy, Vols. 1–3*, Plenum Press, New York, London.
14. A. Kawski (1992) *Photoluminescence of Solutions*, PWN, Warsaw, Chaps 16–19 (in Polish).
15. A. Jabłoński (1960) *Bull. Acad. Polon. Sci. Ser. Sci. Math. Astr. Phys.* **8**, 259.
16. A. Jabłoński (1962) *Bull. Acad. Polon. Sci. Ser. Sci. Math. Astr. Phys.* **10**, 556.
17. F. Perrin (1929) *Ann. Phys. (France)* **12**, 169.
18. R. E. Rose (1957) *Elementary Theory of Angular Momentum*, Wiley, New York.
19. J. Perrin (1926) *2me Conseil de Chim Solvay*, Paris, p. 322.
20. A. Jabłoński (1950) *Acta Phys. Polon.* **10**, 33.
21. A. Jabłoński (1950) *Acta Phys. Polon.* **10**, 193.
22. A. Jabłoński (1965) *Acta Phys. Polon.* **28**, 717.
23. A. Jabłoński (1968) *Bull. Acad. Polon. Sci.* **26**, 601.
24. A. Jabłoński (1977) *Bull. Acad. Polon. Sci.* **25**, 603.
25. R. Bauer, H. Grudziński, A. Jabłoński, and E. Lisicki (1968) *Acta Phys. Polon.* **33**, 803.
26. H. Grudziński (1970) *Acta Phys. Polon.* **A37**, 49.
27. T. P. Gurinovitch, A. M. Sarzevski, and A. N. Sevtchenko (1959) *Opt. Spektr.* **7**, 668.
28. C. Bojarski (1958) *Bull. Acad. Polon. Sci.* **6**, 713.
29. J. Grzywacz (1958) *Bull. Acad. Polon. Sci.* **6**, 705.
30. I. Z. Steinberg (1975) in R. F. Chen and H. Edelhoch (Eds.), *Biochemical Fluorescence Concepts, Vol. 1*, Chap. 3.
31. A. Bączyński, P. Targowski, B. Ziętek, and D. Radomska (1990) *Z. Naturforsch.* **45a**, 618.
32. A. Bączyński, P. Targowski, B. Ziętek, and D. Radomska (1990) *Z. Naturforsch.* **45a**, 1349.
33. A. Bączyński and D. Radomska (1992) *J. Fluoresc.* **2**, 175.
34. A. Bączyński and D. Radomska (1995) *J. Fluoresc.* **5**, 91.
35. T. Azumi and K. Matsuzaki (1977) *Photochem. Photobiol.* **25**, 315.
36. F. E. Williams and M. H. Webb (1951) *Phys. Rev.* **84**, 1181.
37. K. Huang and A. Rhys (1950) *Proc. Roy. Soc.* **A204**, 406.
38. M. Lax (1952) *J. Chem. Phys.* **20**, 1752.
39. S. Kinoshita, N. Nishi, A. Saitoh, and T. Kushida (1987) *J. Phys. Soc. Japan* **56**, 4162.
40. W. Moffit and A. Moscowitz (1959) *J. Chem. Phys.* **30**, 648.
41. B. I. Stepanov (1971) *Izv. Akad. Nauk BSSR, Ser. Phys.-Math.* **3**, 63.
42. B. I. Stepanov (1972) *J. Prikl. Spektrosk.* **17**, 92.
43. W. T. Huntress, Jr (1968) *J. Chem. Phys.* **48**, 3524.
44. T. Tao (1969) *Biopolymers* **8**, 609.
45. L. D. Favro (1960) *Phys. Rev.* **119**, 53.
46. M. Ehrenberg and R. Rigler (1972) *Chem. Phys. Lett.* **14**, 539.
47. T. J. Chuang and K. B. Isenthal (1972) *J. Chem. Phys.* **57**, 5094.
48. A. M. Sarzevski and A. N. Sevtchenko (1971) *Anizotropia Pogloscenia i Ispuskania Sveta*, Chaps. 2–3.
49. A. C. Albrecht (1960) *J. Chem. Phys.* **33**, 156.
50. A. C. Albrecht (1961) *J. Mol. Spectrosc.* **6**, 84.